Fission Fragment Angular Distributions in Charged-Particle-Induced Fission of Ra^{226}†

J. E. GINDLER, G. L. BATE,* AND J. R. HUIZENGA
Chemistry Division, Argonne National Laboratory, Argonne, Illinois
(Received 22 June 1964)

The angular anisotropy of fission fragments from the charged-particle-induced fission of radium has been measured for protons of 10.5-MeV energy and for deuterons and helium ions in the energy ranges from 14 to 21 MeV and 21 to 43 MeV, respectively. A preliminary calculation of the K_0^2 dependence on excitation energy has been made for thorium nuclei of mass 226–230 stretched to the saddle point. (K_0^2 is the average square of the Gaussian distribution in K, the projection of the total angular momentum on the nuclear symmetry axis.) It is shown that the $K_0^2 \propto E^{1/2}$ relation expected on the basis of the Fermi gas model does not hold for excitation energies below some very approximate energy of 16 MeV. Below this energy a $K_0^2 \propto E$ dependence is consistent with the experimental data. The fission cross sections for radium with the projectiles mentioned previously have been measured. These cross sections have been compared with total reaction cross sections calculated on the basis of an optical model with volume absorption. A stepwise increase of the helium-ion-induced fission cross section with projectile energy has been interpreted on the basis of multiple-chance fission. Values of Γ_n/Γ_f have been determined for various thorium nuclei. The magnitude of the so-called "radium anomaly" of fission is shown to be dependent upon the projectile energy at which measurements are made.

I. INTRODUCTION

CONSIDERABLE interest has been displayed in the fission of Ra^{226} because of its anomalous behavior. Radium bombarded with a variety of projectiles of moderate energy gives a fission fragment mass distribution that is triple peaked. This is unlike thorium and elements of greater atomic number that yield mass distributions that are double peaked. It is unlike bismuth and elements of lower atomic number that give mass distributions that are single peaked.

The angular anisotropy of fission fragments measured with respect to an incident beam of charged particles also is anomalous for radium. Compared to the anisotropy of Th^{232}, which appears to be "well behaved," the anisotropy of Ra^{226} is larger for 43-MeV helium ion-induced fission[1,2] and smaller for 21-MeV deuteron-induced fission.[1–3] This anomalous behavior is interpreted on the basis of the temperature of the fissioning nucleus after neutron emission has occurred,[1–4] a large anisotropy being associated with a low nuclear temperature and vice versa.

In the experiments presented herein, the fission fragment anisotropy from a radium target was investigated as a function of the incident energy of deuterons and helium ions. From the results, preliminary calculations were made of the distribution of $\langle K^2 \rangle$ (commonly written K_0^2) with excitation energy, $\langle K^2 \rangle$ being the average square of the Gaussian distribution in K, the projection of the total angular momentum on the nuclear symmetry axis. Fission cross sections were measured for 10.5-MeV protons, for deuterons in the energy range from 14.5 to 21.3 MeV, and for helium ions in the energy range from 20.9 to 42.7 MeV. The fission cross sections measured with deuterons and helium ions were compared to theoretical total reaction cross sections calculated for radium and the respective projectiles. The calculations were based upon an optical model with volume absorption.

II. EXPERIMENTAL

A. General

Charged particles accelerated by the Argonne 60-in. cyclotron were used to induce fission in a radium target centered in an 11-in. scattering chamber. Fission fragments were detected by means of two surface barrier semiconductor detectors located in the chamber at various angles with respect to the beam direction at the target. Pulses from the detectors were amplified, sorted, and ultimately read out from a 256-channel analyzer. Experimental details concerning beam geometry, beam energy calibration and current integration, detector geometries, electronic systems, etc., have been described in the literature[3,5–7] by other workers at this laboratory.

† Based on work performed under the auspices of the U. S. Atomic Energy Commission. An abstract of preliminary results obtained in this work was reported in Bull. Am. Phys. Soc. 7, 303 (1962).

* Present address: Department of Physics, Wheaton College, Wheaton, Illinois.

[1] I. Halpern and C. T. Coffin, *Proceedings of the Second United Nations International Conference on the Peaceful Uses of Atomic Energy, Geneva, 1958* (United Nations, Geneva, 1958), Vol. 15, p. 398.

[2] C. T. Coffin and I. Halpern, Phys. Rev. **112**, 536 (1958).

[3] G. L. Bate, R. Chaudhry, and J. R. Huizenga, Phys. Rev. **131**, 722 (1963).

[4] I. Halpern, Ann. Rev. Nucl. Sci. **9**, 245 (1959).

[5] R. Vandenbosch, H. Warhanek, and J. R. Huizenga, Phys. Rev. **124**, 846 (1961).

[6] J. R. Huizenga, R. Vandenbosch, and H. Warhanek, Phys. Rev. **124**, 1964 (1961).

[7] J. R. Huizenga, R. Chaudhry, and R. Vandenbosch, Phys. Rev. **126**, 210 (1962).

B. Target Preparation

Radium received from the U. S. Radium Corporation was further purified from heavy elements by repeated chemical precipitations as the chloride. A quantity of 239.4 μg of radium was volatilized onto a 0.00025-in.-thick aluminum foil. The foil was masked to give a circular deposit with an area of 1.65 cm^2. The amount of radium on the target was determined by alpha pulse-height analysis in a counter of known low geometry.

The uniformity of the target deposit was investigated. A series of disks was made with each disk having a $\frac{1}{16}$-in.-diam hole drilled in it. The distance from the center of the disk to the center of the hole was different for each disk. These were then used to measure the radium activity of equal areas across the surface of the target. The area that was struck by the cyclotron beam was found to have 1.6 times more radium than the average target thickness. Therefore, a radium thickness of 232 μg/cm^2 was used in the subsequent cross section calculations. The accuracy of this thickness value is estimated to be within $\pm 10\%$.

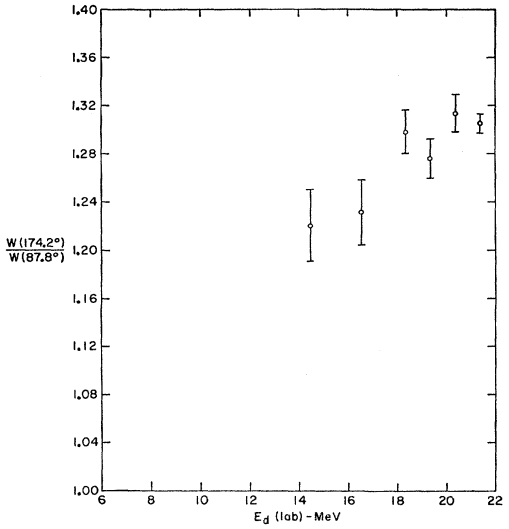

FIG. 1. Deuteron-induced fission fragment anisotropy from radium as a function of projectile energy. The angles given in the differential cross section ratio represent the median center-of-mass angles over the energy range indicated. The errors represent statistical errors combined with errors that result if the measured mean energy of the projectile beam were incorrect to ± 0.2 MeV and the measured mean angle in the laboratory frame of reference were incorrect to $\pm 0.5°$.

III. EXPERIMENTAL RESULTS

A. Energy Dependence of Anisotropy

The anisotropy of fission fragments from the radium target was measured as a function of the energy of the incident deuterons and helium ions and for protons of 10.5-MeV energy. In these experiments the two semiconductor detectors were placed at laboratory reference angles of 86° and 174° for irradiations made with deuterons and helium ions and at 89° and 174° for the one proton irradiation. The angular resolution of the detectors was $\pm 1°$. Data collected for each fissioning system were converted to center-of-mass coordinates assuming (1) full momentum transfer of the incident charged particle to the compound nucleus[8] and (2) equal kinetic energy for all fission fragments. The kinetic energy release in the center-of-mass system was estimated from the relation[9] $\bar{E}_K = 0.121 Z^2/A^{1/3}$ MeV, where $\bar{E}_K$ represents the average total kinetic energy of the fission fragments before neutron emission and Z and A are the atomic and mass numbers, respectively, of the compound nucleus. The measured anisotropy, corrected to the center-of-mass system, for 10.5-MeV proton-induced fission of radium is $W(174.1°)/W(90.0°) = 1.07 \pm 0.03$. The anisotropies measured at various energies for deuteron-induced fission are shown in Fig. 1; for helium-ion-induced fission, in Fig. 2. The angles quoted in the differential cross section ratio in each figure represent the median center-of-mass angles over the energy range indicated. The energy of the incident particle is plotted in the laboratory frame of reference. In the center-of-mass system these energies would be reduced by approximately 1% for deuterons and about 2% for helium ions. The errors shown in Figs. 1 and 2 represent the statistical errors combined with errors that would result if the measured mean energy of the cyclotron beam were incorrect to ± 0.2 MeV and the measured mean angle in the laboratory frame of reference were incorrect to $\pm 0.5°$.

B. Angular Distributions

Detailed angular distributions were obtained for helium-ion-induced fission at 42.4 and 32.7 MeV. One detector was fixed at 190° (170°) with respect to the beam and the other detector was placed at various angles from 86° to 174° in laboratory coordinates. The data were corrected to the center-of-mass frame of reference using the assumptions described in the preceding section. The resulting angular distributions are shown in Fig. 3. The errors indicated are similar to those described for Figs. 1 and 2. The solid curves represent least-squares Legendre polynomial fits[10] of

[8] W. J. Nicholson and I. Halpern, Phys. Rev. **116**, 175 (1959).
[9] J. Terrell, Phys. Rev. **113**, 527 (1959).
[10] H. J. Duffy (private communication).

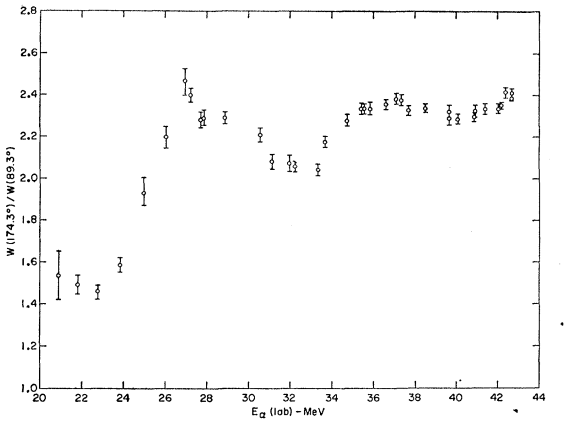

FIG. 2. Helium-ion-induced fission fragment anisotropy from radium as a function of projectile energy. The angles given in the differential cross section ratio represent the median center-of-mass angles over the energy range indicated. The errors represent statistical errors combined with errors associated with projectile energy and detector angle (see description under Fig. 1).

the data

$$W(\theta)/W(90°)=\sum_{i=0}^{n} a_i P_i(\cos\theta).$$

The expansion coefficients a_i obtained by the fitting process are given in Table I. As can be seen from the table, only terms through P_8 at 32.7 MeV and P_{12} at 42.4 MeV have coefficients that are statistically significant. This implies[2,5] that the two angular distributions (Fig. 3) may be accounted for by assuming an

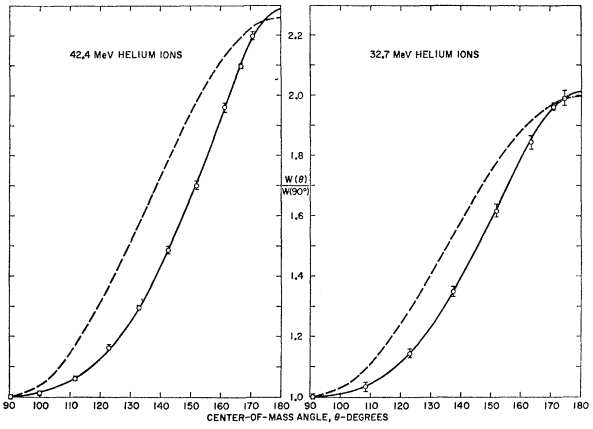

FIG. 3. Angular distributions of fission fragments from the helium-ion-induced fission of raduim. The errors represent statistical errors combined with errors associated with projectile energy and detector angle (see description under Fig. 1). The solid curves represent least-squares Legendre polynomial fits of the data,

$$\frac{W(\theta)}{W(90°)}=\sum_{i=0}^{n} a_i P_i(\cos\theta).$$

The dashed curves represent attempts to fit the data at $\theta=174°$ by the expression $W(\theta)/W(90°)=1+(b/a)\cos^2\theta$.

TABLE I. Angular distributions of fission fragments from 42.4- and 32.7-MeV helium-ion-induced fission of Ra^{226}. The coefficients a_i result from a least-squares fit to the experimental data given in Fig. 3.

a_0	a_2	a_4	a_6	a_8	a_{10}	a_{12}	a_{14}	a_{16}
				32.7 MeV				
1.23091±0.00155	0.58050±0.00314	0.17484±0.00348	0.02469±0.00452					
1.22992±0.00068	0.58077±0.00135	0.16890±0.00175	0.02234±0.00197	0.01508±0.00232				
1.22992±0.00082	0.58077±0.00163	0.16890±0.00207	0.02235±0.00258	0.01508±0.00277	−0.00003±0.00303			
				42.4 MeV				
1.26468±0.00247	0.67339±0.00526	0.24241±0.00577	0.06520±0.00896					
1.26212±0.00141	0.67169±0.00278	0.23889±0.00323	0.06244±0.00490	0.03077±0.00538	0.02086±0.00647			
1.26254±0.00125	0.67298±0.00250	0.23756±0.00288	0.06431±0.00436	0.02969±0.00472	0.02273±0.00571	0.01265±0.00577		
1.26263±0.00137	0.67341±0.00278	0.23857±0.00334	0.06443±0.00479	0.03065±0.00528	0.02144±0.00642	0.01344±0.00638	0.00608±0.00669	
1.26263±0.00175	0.67325±0.00362	0.23809±0.00471	0.06405±0.00632	0.03075±0.00677	0.02124±0.00825	0.01389±0.00837	0.00543±0.00896	−0.00201±0.00839

average orbital angular momentum between the fission fragments of $4\hbar$ and $6\hbar$, respectively. This does not mean that larger l values of orbital angular momentum are excluded in the fission reaction for the following reasons: (1) The angular distribution of fission fragments represents some average orbital angular momentum given by $l\approx(I^2-K^2)^{1/2}$, where I is the angular momentum of the fissioning nucleus and K is the projection of I on the nuclear symmetry axis. (2) Cancellation effects between Legendre functions of higher order makes detection of these terms difficult in an analysis of the fragment angular distribution.

The present fissioning system, $Ra^{226}+He^4$, exhibits more orbital angular momentum between fission fragments than any other helium-ion-induced fissioning system heretofore investigated.[2,5,11] For example, there is no direct evidence for the average l being greater than $3\hbar$ for U^{238}, U^{233}, or Th^{232} bombarded with 42- to 43-MeV helium ions. Only Bi^{209} bombarded with 42.8-MeV helium ions[11] gives any evidence for the average l being as large as 4 to 5 $\hbar$. This further apparent anomaly in radium may be explained by assuming that more fission occurs at low values of K in radium than occurs in the other target nuclides. The magnitude of K is associated directly with the temperature and the moment of inertia of the nucleus. The manner in which low K values are achieved in radium target nuclei is discussed more completely in Sec. IVB.

The average angular momenta brought into radium target nuclei by 42.4- and 32.7-MeV helium ions are approximately 15 $\hbar$ and 11 $\hbar$, respectively. These momenta are considerably larger than the orbital angular momenta exhibited between fragments in the respective angular distributions. The difference between the two depends largely upon the values of K available. In view of the analysis of the K_0^2 distribution made in Sec. IV B, one might reasonably expect larger average orbital angular momenta than those observed. If neutrons emitted before fission carry away little angular momentum, then the fission fragments of the ($Ra^{226}+He^4$) system should be formed with moderately large spins. No direct experimental information is presently available for this particular system. However, it has been shown[12–14] that in the formation of isomeric pairs produced by the irradiation of uranium nuclides with helium ions, the yield of the high spin isomer relative to that of the low-spin isomer increases as the helium ion energy is increased from 30 to 40 MeV.

[11] R. Chaudhry, R. Vandenbosch, and J. R. Huizenga, Phys. Rev. **126**, 220 (1962).
[12] L. J. Colby, M. L. Shoaf, and J. W. Cobble, Phys. Rev. **121**, 1415 (1961).
[13] H. Münzel, Nukleonik **3**, 58 (1961).
[14] R. Vandenbosch and H. Warhanek, J. Inorg. Nucl. Chem. (to be published).

The dashed curves in Fig. 3 represent attempts to fit the helium-ion-induced fission data by the expression

$$W(\theta)/W(90°)=1+(b/a)\cos^2\theta. \quad (1)$$

The data at $W(174°)/W(90°)$ were used to determine the coefficient b/a. As can be seen from the figure, such an expression does not represent the data very well. Equation (1) also has been found to represent rather poorly angular distributions obtained from helium ion-induced fission of other nuclides.[6,7] However, Eq. (1) has been found to represent quite well the angular distributions obtained from deuteron-induced fission of various nuclides.[3] It has, therefore, been assumed that the angular distribution of deuteron-induced fission fragments from radium can also be represented by an equation of this type.

C. Fission Cross Sections

Fission cross sections in terms of cm^2 were calculated according to the equation

$$\sigma_F=\frac{1}{FN}\frac{C_{90}}{\omega_d}\int_0^{2\pi}\frac{W(\theta)}{W(90°)}d\omega, \quad (2)$$

where F is the integrated number of bombarding particles, N is the number of radium target nuclei per cm^2, C_{90} is the number of counts detected at 90° in the center-of-mass coordinate system, ω_d is the solid angle subtended by the 90° detector, $W(\theta)/W(90°)$ is the center-of-mass angular distribution for the particular energy of the charged particle involved, and the integration is made over 2π steradians. For proton- and deuteron-induced fission, an angular distribution typified by Eq. (1) was used. A similar expression was used for helium-ion-induced fission. However, a correction was applied to the integrated cross section expression, Eq. (2), to make it correspond to the integration of the fitted Legendre polynomial (Fig. 3). The correction was derived in the following manner: The expressions describing the solid and dashed curves in Fig. 3 were integrated over 2π solid angle. The ratio of these two integrated expressions, solid/dashed, was then plotted as a function of the measured anisotropy, $W(174°)/W(90°)$, and a straight line drawn between the two points. Corrections to the integrated cross sections were then applied on the basis of the measured anisotropy. For anisotropies $W(174°)/W(90°)$ of 1.0 and 2.4 the corrections applied were 0.998 and 0.897, respectively. Similar corrections have been applied to the calculation of cross sections for helium-ion-induced fission of uranium,[6] gold, and bismuth.[7] The value of these latter corrections varied from 0.93 and 0.95 for U^{233} irradiated with 41.7- and 32-MeV helium ions, respectively, to 0.89 and 0.88 for gold and bismuth, respectively, irradiated with 42.8-MeV helium ions. An estimate of

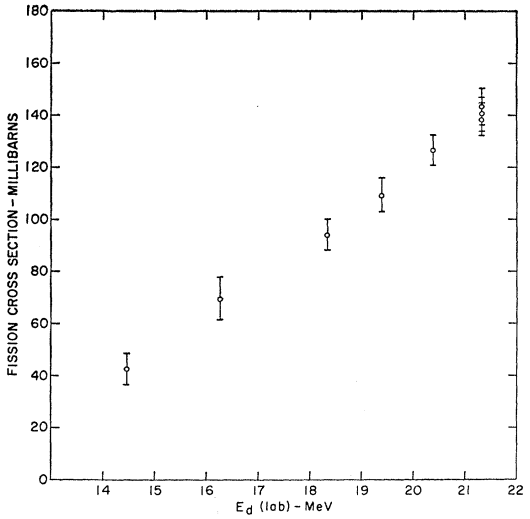

FIG. 4. Deuteron-induced fission cross sections of radium as a function of projectile energy. The statistical errors are indicated.

the error associated with the application of these corrections to the present cross section calculations is $\pm 4\%$.

The calculated fission cross section of Ra^{226} with 10.5-MeV protons is 4.6 ± 1.1 mb. Excitation functions for the fission of Ra^{226} with deuterons and helium ions are given in Figs. 4 and 5, respectively. The particle energy quoted above and shown as the abscissas in Figs. 4 and 5 is expressed in laboratory coordinates. Data are plotted for an assumed monoenergetic cyclotron beam. Each energy is taken as the mean value of the energy distributions. Measurements of the energy spread of the deuteron beam at the Argonne 60-in. cyclotron[15] indicate a full width at half-maximum of less than 0.2 MeV at 21MeV and 0.4 MeV at 14 MeV. Similar measurements have not been made for the helium ion beam as a function of energy. However, the full width at half-maximum intensity of the elastically scattered peak of the 43-MeV helium ion beam has been measured to be ≤ 0.35 MeV.[16] Combining this with calculations of the energy spread introduced by the energy loss of helium ions in aluminum absorbers gives a full width at half-maximum intensity of 0.8 MeV for a 20-MeV helium-ion beam.[6] The true fission cross sections may therefore vary somewhat from the values calculated for an assumed monoenergetic cyclotron beam depending upon the cross section versus projectile energy relation and upon the distribution of the projectile energy.

The error quoted for the 10.5-MeV proton cross section and the errors shown in Figs. 4 and 5 represent statistical errors. Absolute errors may be estimated by combining the statistical errors with estimated standard errors of 12% for the helium ion and deuteron cross sections and 25% for the proton cross section. These latter errors are compounded from errors in the determination of target thickness, anisotropy correction, dead-time corrections, solid-angle subtended by the solid-state detectors, angular positions, and integrated projectile flux.

Jensen and Fairhall[17,18] have measured radiochemically the fission cross sections of Ra^{226} resulting from proton, deuteron, and helium ion bombardments. Their results are listed in Table II, second column. These authors estimate their fission cross sections to be accurate probably within a factor of about 2. Corresponding cross sections taken from the present work are listed in the third column of Table II. The ratios of the two results are given in column four. As can be seen from this last column, present results are generally a factor of 2 to 4 greater than the radiochemical results.

TABLE II. A comparison of measured fission cross sections for Ra^{226}.

Projectile and energy	Fission cross section (mb) σ_1[a]	σ_2[b]	σ_2/σ_1
10.5-MeV p	2 ± 1	4.6 ± 1.5	2.3 ± 1.4
14.5-MeV d	12	43	3.6
21.5-MeV d	80	140	1.8
23.5-MeV α	10	70	7
31 -MeV α	100	410	4.1
43 -MeV α	310	940	3.0

[a] Reference 18.
[b] Present work.

IV. DISCUSSION

A. Cross Sections

The $Ra^{226}(He^4,f)$ excitation function (Fig. 5) is unusual in that it increases in a stepwise manner as

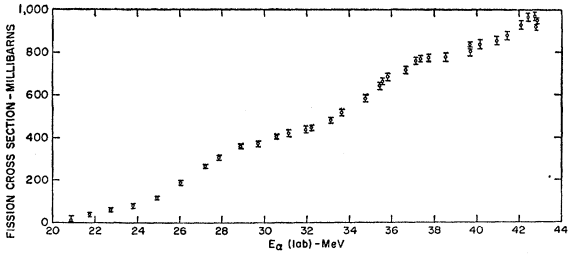

FIG. 5. Helium-ion-induced fission cross section of radium as a function of projectile energy. Statistical errors are indicated.

[15] W. J. Ramler, J. L. Yntema, and M. Oselka, Nucl. Instr. Methods 8, 217 (1960).
[16] B. Wilkins (private communication).
[17] R. C. Jensen and A. W. Fairhall, Phys. Rev. 109, 942 (1958).
[18] R. C. Jensen and A. W. Fairhall, Phys. Rev. 118, 771 (1960).

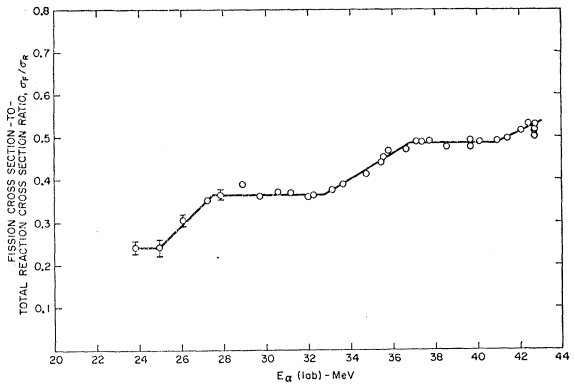

FIG. 6. The ratio of fission cross section to total reaction cross section for radium as a function of helium ion energy. The total reaction cross section was calculated on the basis of an optical model with volume absorption. The errors shown represent errors in the fission cross section only (see description under Fig. 1).

the helium ion energy is increased. This stepwise increase has not been observed heretofore in charged-particle-induced fission excitation functions (see, for example, Refs. 3, 6, 7, 19, 20). It has been observed for neutron-induced fission excitation functions[21] in the MeV-neutron energy range. The stepwise increase in the fission cross section with increased neutron energy is associated with multiple-chance fission. That is, as the neutron energy is increased, fission can occur by $(n,n'f)$, $(n,n'n''f)$, etc., reactions as well as the (n,f) reaction. The former reactions are referred to as 2nd-, 3rd-, etc., chance fission. As each of these reactions becomes energetically possible, the total fission cross section exhibits a sudden increase. This increase is followed by a leveling off of the total fission cross section until another later-chance fission reaction becomes energetically possible.

The stepwise variation in the $Ra^{226}(He^4,f)$ excitation function is more visibly pronounced if the fission cross section to total reaction cross section ratio, σ_F/σ_R, is plotted against the energy of the incoming helium ion. This is displayed in Fig. 6. The total reaction cross section was calculated on the basis of a volume-absorption optical model.[22] The Woods-Saxon parameters, $V=-50$ MeV, $W=-25.3$ MeV, $R=1.17A^{1/3}+1.77$ F, and $d=0.576$ F were used in the calculation.

The stepwise character of the σ_F/σ_R versus E_α curve may be explained on the basis of competition between fission and neutron emission. If one assumes that (1) charged-particle emission is negligible compared to fission and neutron emission and that (2) gamma-ray emission does not compete favorably with the latter two processes at energies above the thresholds for fission or neutron emission, then the ratio σ_F/σ_R may be expressed in terms of the ratios $\Gamma_f/(\Gamma_f+\Gamma_n)$ for the various fissioning nuclei and their probabilities for appearing. In this expression, $\Gamma_f/\hbar$ and $\Gamma_n/\hbar$ represent the partial fission and neutron probabilities of decay, respectively. A 24-MeV helium ion captured by a Ra^{226} nucleus results in a Th^{230} nucleus excited to approximately 19 MeV.[23] This nucleus, according to the above considerations can either (1) fission, (2) emit a neutron and then fission, or (3) emit two neutrons and then continue the de-excitation process by the emission of gamma rays. As the energy of the incoming helium ion is increased to >25 MeV, third-chance fission (fission following the emission of two neutrons) becomes possible. However, at this energy third-chance fission is not possible for all Th^{230} compound nuclei that were excited initially and had emitted two neutrons. This results from the fact that neutrons carry away various amounts of kinetic energy and leave the residual nuclei at different levels of excitation. Consequently, at $E_\alpha=25$ MeV some of the residual Th^{228} nuclei have sufficient energy to fission while others do not. As the energy of the incoming helium ion is increased, however, more and more of the residual Th^{228} nuclei have sufficient excitation energy either to fission or to emit another neutron. With 27.5-MeV helium ions, essentially all of these Th^{228} nuclei have enough energy to de-excite by either process. The residual Th^{227} nuclei formed by neutron emission of the Th^{228} nuclei do not have sufficient energy either to fission or to emit a neutron. The σ_F/σ_R curve therefore levels off and remains level to about 32-33 MeV. At this point fourth-chance fission becomes energetically possible and the value of σ_F/σ_R again increases.

The competition between fission and neutron emission is illustrated in Fig. 7. The number of nuclei shown to de-excite by either fission or neutron emission has been calculated on the basis of the σ_F/σ_R values exhibited in the plateau regions of Fig. 6. For example, according to Fig. 6, with helium ions of 23- to 24-MeV energy, 24.1% of the total reaction cross section is involved in fission. Since the plateau at this energy represents the sum of first- and second-chance fission, the number of Th^{230} and Th^{229} nuclei that fission should

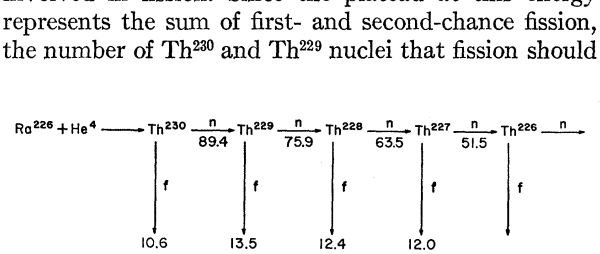

FIG. 7. Neutron emission-fission competition in thorium nuclei formed by the bombardment of radium with helium ions.

[19] J. Jungerman, Phys. Rev. **79**, 632 (1950).
[20] G. H. McCormick and B. L. Cohen, Phys. Rev. **96**, 722 (1954).
[21] D. J. Hughes and R. B. Schwartz, BNL 325, July 1950, 2nd ed. 1950 (unpublished).
[22] J. R. Huizenga and G. Igo, ANL 6373, 1961 (unpublished); Nucl. Phys. **29**, 462 (1962).
[23] Calculated on the basis of the relative nuclidic masses compiled by F. Everling, L. A. König, J. E. Mattauch, and A. H. Wapstra, Nucl. Phys. **18**, 529 (1960).

be 24.1 of every 100 Th^{230} nuclei originally formed. This number is indicated in Fig. 7. At the second plateau of Fig. 6, 36.5% of the original Th^{230} nuclei de-excite via fission. At this energy first-, second-, and third-chance fission may occur. Consequently, 36.5−24.1 or 12.4 Th^{228} nuclei undergo fission for every 100 Th^{230} nuclei formed. Similar reasoning is used to calculate the neutron emission-fission competition in residual Th^{227} nuclei. The numbers indicated in Fig. 7 for neutron emission and fission of Th^{230} and Th^{229} nuclei were calculated in the following manner. Values of Γ_n/Γ_f have been compiled[24,25] for a number of nuclides at low and moderate excitation energies. Values of 7.8 and 5.1 are estimated for the two nuclides, Th^{230} and Th^{229}, respectively. Using these estimates of Γ_n/Γ_f, an 11.4% value of $\Gamma_F/(\Gamma_F+\Gamma_N)$ is obtained for first-chance fission and 25.9% for first- plus second-chance fission. The latter value is about 7% larger than the 24.1% indicated in Fig. 6. Therefore, the calculated number of fission events occurring by first- and by second-chance fission was reduced by 7%. New Γ_n/Γ_f values were then calculated from this lower number.

Values of Γ_n/Γ_f for the various thorium nuclides calculated by the above analysis are given in Table III.

TABLE III. Γ_n/Γ_f ratios for thorium nuclides.

Th^{230}	Th^{229}	Th^{228}	Th^{227}	Reference
8.4	5.6	5.0	3.8	Present work
7.8	5.1	3.4		24, 25
8.2	6.4	4.6	3.4	1

The errors associated with these values are ~12%, the estimated absolute errors of the fission cross sections. Values of Γ_n/Γ_f taken from the straight-line plot of Ref. 24 or 25 and from a smooth curve plotted through the data presented in Ref. 1 are given for comparison.

The present values of Γ_n/Γ_f given in Table III were calculated on the assumption that they were independent of both excitation energy and angular momentum. The fact that the ratio σ_F/σ_R (Fig. 6) proceeds stepwise with energy tends to support this argument. At least the excitation energy and angular momentum dependencies of Γ_n/Γ_f appear to be so very small that they cannot be detected in the range of energies involved.

The effect of excitation energy and angular momentum upon the Γ_n/Γ_f ratio may be calculated theoretically. Using Eq. (15) of Ref. 25, which assumes a Fermi gas level density of the excited nucleus, the value of Γ_n/Γ_f for Th^{230} is calculated to increase slightly (~1.5×) from 21- to 43-MeV helium ion excitation of radium. On the other hand, the value of Γ_n/Γ_f for Th^{229} is calculated to increase well over an order of magnitude (~40×) in this same energy range. Since Th^{229} results from neutron evaporation of Th^{230} formed by helium-ion excitation of Ra^{226}, its excitation energy is very low when the energy of the helium ions is only 21 MeV. It is in this region of low excitation that the value of Γ_n/Γ_f is theoretically predicted to change most with energy. Therefore, even though the predicted change in Γ_n/Γ_f for Th^{229} is rather large over the energy range of 21- to 43-MeV helium ions, most of the change is expected to occur within the first few MeV (~20× from 21- to 29- MeV helium-ion energy). If, rather than Eq. (15), one uses Eq. (16) of Ref. 25, which assumes a constant temperature level density of the excited nucleus, then a decrease in the Γ_n/Γ_f ratio for both Th^{230} and Th^{229} in the helium ion energy range stated above is indicated because of rotational energy effects. The amount of decrease thus indicated depends upon the nuclear temperature used in the calculation (~0.5× for $\tau=1$ MeV; ~0.3× for $\tau=2$ MeV). The decrease in Γ_n/Γ_f predicted for both Th^{230} and Th^{229} is about the same. From the experimental results it appears that a theoretical expression for Γ_n/Γ_f is most appropriate in which the density level of the excited nucleus is described by a constant nuclear temperature at low excitation energies and by a Fermi gas at higher excitation energies.

Figure 8 depicts the variation of the deuteron-induced fission cross section to total reaction cross section ratio with deuteron energy. In this case, the increase in the ratio with increasing deuteron energy is monotonic rather than stepwise. The absence of any step function

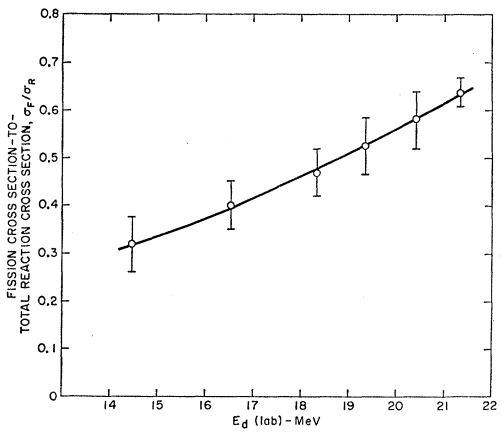

FIG. 8. The ratio of fission cross section to total reaction cross section for radium as a function of deuteron energy. The total reaction cross section was calculated on the basis of an optical model with volume absorption. The limits of errors represent statistical and systematic errors in the fission cross section only.

[24] J. R. Huizenga and R. Vandenbosch, *Proceedings of the Second United Nations International Conference on the Peaceful Uses of Atomic Energy, Geneva, 1958* (United Nations, Geneva, 1958), Vol. 15, p. 284.

[25] J. R. Huizenga and R. Vandenbosch, in *Nuclear Reactions*, edited by P. M. Endt and P. B. Smith (North-Holland Publishing Company, Amsterdam, 1962), Vol. II, Chap. II.

may be the result of a change in the energy dependence of Γ_n/Γ_f between thorium and actinium or it may be the result of limitations in the experimental measurements. The latter may mask any stepwise character in the σ_F/σ_R curve for the following reasons: (1) The deuteron energy range is limited from 14.5 to 21.3 MeV. This range is roughly equivalent to the binding energy of a neutron with less than 1 MeV of kinetic energy. As a result, only one or perhaps two plateaus in a step function may be anticipated, depending upon where they occur in the energy range covered. (2) The statistics are not as good for the deuteron data as they are for the helium ion data. Therefore, the relative errors of the deuteron data shown in Fig. 8 do not negate the possibility of a plateau. (3) The data were taken at intervals of 2 to 4 MeV. Energy intervals of ≤ 1 MeV would be more conducive to the determination of whether or not a plateau does exist.

B. Fission Fragment Anisotropy

The anisotropy versus helium ion energy curve (Fig. 2) has features similar to those obtained for helium ion-[5] and neutron-induced[26,27] fission of other target nuclides. That is, there is a general increase in anisotropy with increasing projectile energy. Imposed upon this curve are sharp increases in anisotropy. The resulting curve is one in which the anisotropy may exhibit wide variations with projectile energy.

The general features of these anisotropy versus projectile energy curves have been explained by the theory advanced by Bohr[28] and amplified by Strutinskii,[29–33] Halpern and Strutinskii,[34] Griffin[35,36] and others. According to this theory, the angular distribution $W(\theta)$ of fission fragments emitted per unit solid angle for a single fissioning species is described by the relation,

$$W(\theta)\sim\int dI\int dK\, f(K,I)[\sin^2\theta-(K^2/I^2)]^{-1/2}, \quad (3)$$

where θ is the direction of fission fragments with respect to the beam direction, I is the angular momentum of the compound state, and K is the component of angular moment along the symmetry axis. With the assumptions (1) that $f(K,I)$ is a product of the functions $f_K(K)$ and $f_I(I)$, (2) that $f_K(K)$ can be represented by a Gaussian distribution with $f_K(K)\sim\exp(-K^2/2K_0^2)$ and (3) that $f_I(I)\sim I$ up to some limiting value[5] I_m, then the integration of Eq. (3) results in an expression dependent upon K_0 and I_m. Both $W(\theta)$ and the ratio $W(\theta)/W(90°)$ may be characterized by the parameter $P=(I_m/2K_0)^2$.

At high excitation energies, statistical arguments[35] predict that K_0^2 is proportional to the square root of the excitation energy at the saddle point. I_m^2, taken to be equal[5] to $2\langle I^2\rangle_{\text{av}}$, exhibits a nearly linear dependence upon the bombarding energy of the helium ions from 23- to 43-MeV. Consequently, because of the $(I_m/2K_0)^2$ dependence of angular anisotropy a general increase may be expected with increasing helium ion energy and, hence, excitation energy for a particular fissioning species.

As indicated previously, Ra^{226} excited with 43-MeV helium ions is capable of undergoing fifth-chance fission. That is, not only is the compound nucleus Th^{230} contributing to the fission fragment anisotropy but so are Th^{229}, Th^{228}, Th^{227}, and Th^{226} nuclei (see Fig. 7). The resulting angular distribution may then be expressed as a sum of the angular distributions of the contributing fissioning species,

$$W_{\text{resultant}}(\theta)=\textstyle\sum_i \alpha_i W_i(\theta,I_m^{(i)},K_0^{(i)}), \quad (4)$$

where α_i is the fractional contribution of a particular fissioning species to the total number of fission events at a particular angle θ and a particular bombarding energy.

If the amount of angular momentum carried away by evaporated neutrons is very small compared to the angular momentum of the compound system, then I_m^2 may be considered approximately constant for all fissioning species. However, the excitation energy and hence K_0^2 of the fissioning nucleus change greatly with the number of neutrons emitted prior to fission. Therefore, at an excitation energy that is low, that is, one slightly above the threshold energy of ith-chance fission, the angular anisotropy $W_i(\theta)/W_i(90°)$ for that particular ith-chance fission should be large. This large anisotropy is then superimposed upon the anisotropies resulting from $(i-1)$-, $(i-2)$-, $\cdots$, 1-chance fission. If the contribution of these latter fissioning species to the total anisotropy is small compared to that of the ith-fissioning species, then a large increase in anisotropy is expected. Otherwise only a small anisotropy change may be expected.

Since the magnitude of the anisotropy is largely dependent upon the value of K_0^2, it becomes important to know how this quantity varies as a function of the excitation energy. Statistical considerations coupled

[26] L. Blumberg and R. B. Leachman, Phys. Rev. **116**, 102 (1959).
[27] J. E. Simmons and R. L. Henkel, Phys. Rev. **120**, 198 (1960).
[28] A. Bohr, *Proceedings of the International Conference on the Peaceful Uses of Atomic Energy, Geneva, 1955* (United Nations, New York, 1956), Vol. 2, p. 151.
[29] V. M. Strutinskii, Zh. Eksperim. i Teor. Fiz. **30**, 606 (1956) [English transl.: Soviet Phys.—JETP **3**, 638 (1956)].
[30] V. M. Strutinskii, Atomnaya Energ. **2**, 508 (1957) [English transl.: Soviet J. At. Energy **2**, 621 (1957)].
[31] V. M. Strutinskii, Zh. Eksperim. i Teor. Fiz. **39**, 781 (1960) [English transl.: Soviet Phys.—JETP **12**, 546 (1961)].
[32] V. M. Strutinskii, Zh. Eksperim. i Teor. Fiz. **40**, 933 (1961) [English transl.: Soviet Phys.—JETP **13**, 652 (1961)].
[33] V. M. Strutinskii, Zh. Eksperim. i Teor. Fiz. **40**, 1794 (1961) [English transl.: Soviet Phys.—JETP **13**, 1261 (1961)].
[34] I. Halpern and V. M. Strutinskii, *Proceedings of the Second United Nations International Conference on the Peaceful Uses of Atomic Energy, Geneva, 1958* (United Nations, Geneva, 1958), Vol. 15, p. 408.
[35] J. Griffin, Phys. Rev. **116**, 107 (1959).
[36] J. Griffin, Phys. Rev. **127**, 1248 (1962).

with a Fermi gas model give

$$K_0^2 = t\mathcal{I}_{\text{eff}}/\hbar^2, \quad (5)$$

where t is the thermodynamic temperature and $\mathcal{I}_{\text{eff}}$ is the effective moment of inertia. The latter is defined as $\mathcal{I}_{\text{eff}} = \mathcal{I}_\perp \mathcal{I}_\parallel / (\mathcal{I}_\perp - \mathcal{I}_\parallel)$, where $\mathcal{I}_\perp$ is the moment of inertia perpendicular to the symmetry axis and $\mathcal{I}_\parallel$ is the moment of inertia parallel to the symmetry axis. According to the Fermi gas model, $t \sim E^{1/2}$, where E is the excitation energy. Therefore,

$$K_0^2 \sim E^{1/2}\mathcal{I}_{\text{eff}}/\hbar^2. \quad (6)$$

Analyses of experimental data[5,27,37,38] indicate that for comparable values of $\mathcal{I}_{\text{eff}}$, K_0^2 is actually lower than the values predicted by expression (6) for low excitation energies. Griffin[37] has shown that from $E=0$ up to some critical value E_c, experimental data are fitted nicely by a linear dependence of K_0^2 upon E. For excitation energies greater than E_c the square-root dependence of relation (6) appears to become valid.

In the present paper, various distributions of K_0^2 with excitation energy have been assumed in an effort to fit the experimental data of Fig. 2. In order to make the necessary calculations, the following assumptions have been made:

(1) The anisotropy $W(174°)/W(90°)$ is given by the quotient of two expressions where each expression may be represented by Eq. (4). $W(174°)$ and $W(90°)$ normalized to unit fission were computed according to Eq. (3). The assumptions made concerning the $f(K,I)$ distribution are outlined in the discussion following Eq. (3).

(2) $I_m^2 = 2\langle I^2\rangle_{\text{av}}$.[5] The dependence of $\langle I^2\rangle_{\text{av}}$ on bombarding energy was determined from optical-model barrier transmission coefficients.[22]

(3) I_m^2 does not effectively change with the evaporation of neutrons prior to fission.

(4) Values of α_i were determined from the values of Γ_n/Γ_f described in the previous section.

(5) The excitation energy E_k of the kth fissioning nucleus at the saddle point was calculated following the development of Lang[39] by the relation:

$$E_k = \frac{A}{8}t^2 - t = E_\alpha + Q - \left(\sum_{i=1}^{k-1} B_{n_i} + 2\sum_{i=2}^{k}\tau_i\right) - E_{f_k} - \Delta_k, \quad (7)$$

where A is the mass of the fissioning nucleus, t is the thermodynamic temperature [for calculating K_0^2 as in Eq. (5)], E_α is the energy of the bombarding helium ion in the center-of-mass system, Q is the energy of reaction for the formation of the compound nucleus,[23] B_{n_i} is the neutron binding energy[23] of the last neutron of the ith nucleus, τ_i is the nuclear temperature (used to calculate the amount of kinetic energy carried away by neutron evaporation) of the ith nucleus, E_{f_k} is the fission threshold of the kth nucleus, and Δ_k is the pairing energy of the kth nucleus determined from ground state mass differences. The subscripts $i=1, 2, 3, \cdots$ refer to Th^{230}, Th^{229}, Th^{228}, $\cdots$ nuclides, respectively.

Δ_k was calculated from the relation[40,41]

$$\begin{aligned}\Delta_k &= 1.68 - 0.0042A \quad \text{for odd-}A\text{ compound nuclei}\\ &= 2(1.68 - 0.0042A)\\ &\qquad \text{for even-}A\text{, even-}Z\text{ compound nuclei.}\end{aligned} \quad (8)$$

E_{f_k} was calculated from the empirical relation given by Eq. (8) of Ref. 7. It is assumed that Δ_k for the saddle point does not differ substantially from the value of Δ_k for the ground state. The empirical relation for E_{f_k} does not contain the pairing energy correction explicitly accounted for by the inclusion of Δ_k in Eq. (7).

The nuclear temperature was calculated from the equation,

$$\frac{A}{8}\tau_k^2 - 4\tau_k = E_\alpha + Q - \left(\sum_{i=1}^{k-1} B_{n_i} + 2\sum_{i=2}^{k}\tau_i\right) - \Delta_k. \quad (9)$$

A plot of the average excitation energy E_k versus helium ion energy E_α(lab) results in a straight line for each particular thorium nuclide k. In the E_α(lab) range from 21 to 43 MeV, Th^{228}, Th^{227}, and Th^{226} have saddle-point excitation energy thresholds according to Eq. (7) at helium ion energies of 26.2, 34.6, and 42.5 MeV, respectively. As can be seen from Fig. 6, these helium ion energies do not correspond to the onset of third-, fourth-, and fifth-chance fission as previously described. This discrepancy in "fission thresholds" may be accounted for by the realization that the calculated values of E_k represent average saddle point excitation energies but that neutrons are emitted from the excited thorium nuclides with a spectrum of excitation energies. This results in a spectrum of excitation energies for a particular thorium nuclide at a specific helium ion energy. The onset of fission preceding the calculated fission threshold may be attributed to those nuclides having excitation energies greater than the average. This difference between observed and calculated fission thresholds was compensated for in the following manner. The calculated saddle point excitation energy was assumed to hold in the plateau regions of the σ_F/σ_R versus E_α (lab) curve shown in Fig. 6. In the regions of 24.9–27.5 MeV, 32.8–36.8 MeV, and 40.8–upward MeV, in which the σ_F/σ_R ratio is changing, an effective excitation energy was used for the three thorium nuclides: 228, 227, and 226, respectively. This effective excitation energy was taken to be zero at the smaller helium ion energy (24.9, 32.8, and 40.8 MeV for the respective

[37] J. Griffin, Phys. Rev. **132**, 2204 (1963).
[38] H. C. Britt, R. H. Stokes, W. R. Gibbs, and J. J. Griffin, Phys. Rev. Letters **11**, 343 (1963).
[39] D. W. Lang, Nucl. Phys. **26**, 434 (1961).
[40] T. D. Newton, Can. J. Phys. **34**, 804 (1956).
[41] A. Stolovy and J. A. Harvey, Phys. Rev. **108**, 353 (1957).

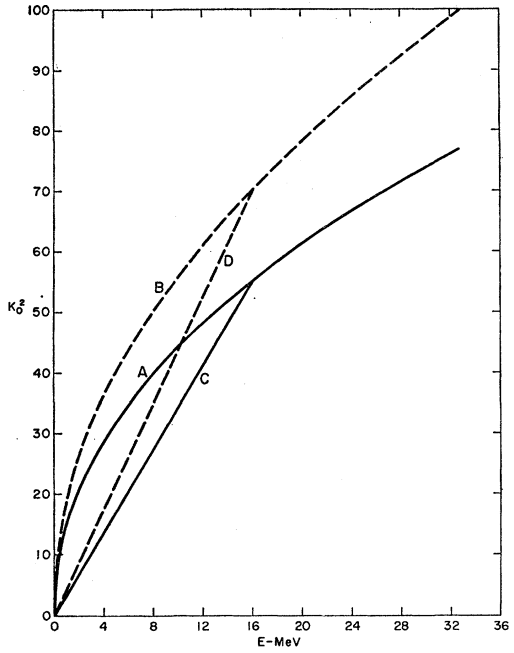

FIG. 9. Variation of K_0^2 with saddle point excitation energy for thorium nuclei with mass 266-230. The four K_0^2 versus E distributions were used to calculate the respective $W(174°)/W(90°)$ versus E_α(lab) curves shown in Figs. 10 and 11. The various assumptions which the above curves represent are described in the text.

thorium nuclides) and to increase linearly with helium ion energy until it intersects the calculated E_k versus E_α(lab) curve at the larger helium ion energy.

The various functions of $K_0^2(E)$ used to calculate the angular anisotropies are shown in Fig. 9. (The variable E is now used to denote excitation energy previously denoted by E_k; the subscript labeling the particular fissioning nucleus is dropped for the more general considerations to follow). Curves A and B represent functions of the type given by Eq. (6). In curve A, $\mathcal{I}_{\text{eff}}$ was taken as the value calculated by Cohen and Swiatecki[42] and Strutinskii *et al.*,[43] on the basis of a uniformly charged liquid drop for a fissionability parameter $X=(Z^2/A)/50.13$, of 0.7 (see Fig. 13 of Ref. 3). In curve B, $\mathcal{I}_{\text{eff}}$ was obtained by interpolation of the experimental results (Fig. 13 of Ref. 3) to a fissionability parameter of 0.7. Curves C and D represent K_0^2 as a linear function of E up to some arbitrarily chosen value of E beyond which the two curves become identical with curves A and B, respectively.

The results of the various calculations are shown in Fig. 10. The experimental results are shown also for comparison. As can be seen from the figure, K_0^2 distributions represented by curves A and B in Fig. 9 do not fit the experimental data very well. Although these K_0^2 distributions give rise to angular anisotropies that increase with increasing helium ion energy, the increase is almost stepwise. The sharp increases represented by the experimental data are absent. The K_0^2 distributions represented by curves C and D of Fig. 9, however, lead to angular aniostropies that represent rather well the general features of the experimental data. Considering the number of assumptions made in the calculations, the results are both rather amazing and gratifying. The largest discrepancy in the over-all features between the experimental and calculated values of the anisotropy appears to be in the region of 35 MeV, the region in which fourth-chance (Th^{227}) fission becomes possible. The calculated anisotropies indicate a sharp increase in this energy region. The experimental results do not reflect this. Since the excitation energy of Th^{227} is very low at 35 MeV, K_0^2 from curves C and D of Fig. 9 is also low. However, Th^{227} is an odd-A nuclide which in its ground state should not have $K_0^2=0$ but some finite value[37] $\langle k^2\rangle_{\text{av}}$. Therefore, the anisotropies resulting from K_0^2 distributions A, C, and D in Fig. 9 were recalculated by adding $\langle k^2\rangle_{\text{av}}=10$ to the K_0^2 values of all odd-A (Th^{227} and Th^{229}) fissioning nuclides. The results of these latter calculations are given in Fig. 11. Each of the curves, A′, C′, and D′, in the figure represents a lower anisotropy than its corresponding curve in Fig. 10. However, the large spikes present in curves C and D at 35 MeV in Fig. 10 are either almost or completely missing from curves C′ and D′ in Fig. 11. Curves C in Fig. 10 and C′ in Fig. 11 bracket the high-energy experimental data rather well up to the point where fifth-chance fission becomes energetically possible. A judicious choice of $\langle k^2\rangle_{\text{av}}$ may give calculated values of the anisotropy that fit the experimental data quite well.

From the results of the above calculations it appears that K_0^2 does not exhibit a parabolic dependence

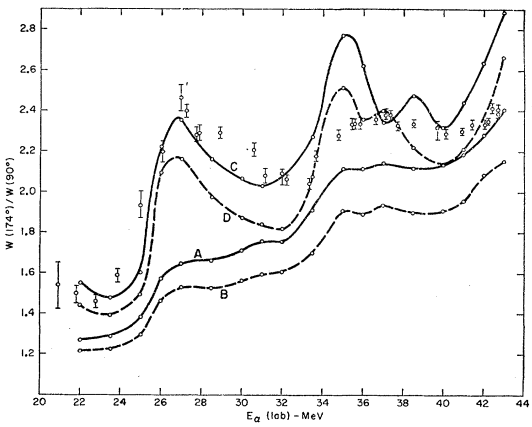

FIG. 10. Theoretical fits to the energy dependence of the helium-ion-induced fission fragment anisotropy of radium. Curves A through D result from the respective K_0^2 versus E distributions shown in Fig. 9.

[42] S. Cohen and W. J. Swiatecki, Ann. Phys. (N. Y.) **19**, 67 (1962).

[43] V. M. Strutinskii, N. Ya. Lyaschenko, and N. A. Popov, Zh. Eksperim. i Teor. Fiz. **43**, 584 (1962) [English transl.: Soviet Phys.—JETP **16**, 418 (1963)]; Nucl. Phys. **46**, 639 (1963).

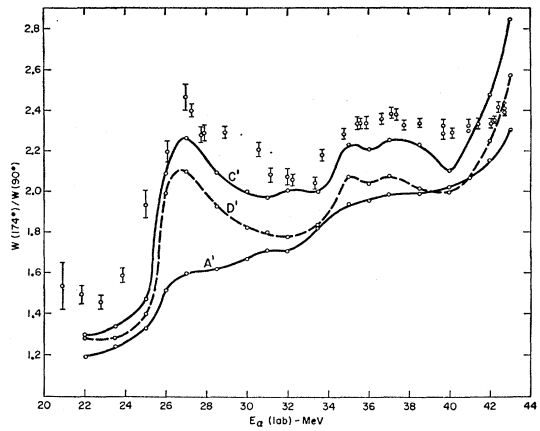

FIG. 11. Theoretical fits to the energy dependence of the helium-ion-induced fission fragment anisotropy of radium. Curves A' through D' result from the respective K_0^2 versus E distributions shown in Fig. 9 but modified for odd-A thorium nuclei. The modification results in larger K_0^2 values for these nuclei at a particular excitation energy (see text).

[Eq. (6)] on excitation energy at lower excitation energies. This is consistent with other experimental results.[5,27,37,38] The hypothesis of a linear dependence of K_0^2 upon E from $E=0$ to $E=E_c$, the critical value of E, is not inconsistent with the present experimental data. It is obvious that another choice of E_c may change the calculated anisotropies appreciably. Theoretically E_c is dependent upon the level density parameter a and the square of the ground-state value of the energy gap parameter θ_0 i.e., $E_c=0.48a\theta_0^2$. A recent study[44] has shown θ_0 to be about 1.3 times the pairing energy parameter Δ_k as determined for an odd-A nucleus according to Eq. (8). If one takes $a=A/8$ MeV^{-1}, the critical energy calculated for Th^{228} is then 12 MeV. A somewhat larger value of 15.2 MeV is calculated for E_c if one uses the formulation of Nemirovsky and Adamchuk[45] to obtain Δ_k. Griffin[37] has placed the value of E_c between 18.3 and 19.6 MeV for plutonium nuclides. This was done on the basis of fission experiments with compound nuclei of Pu^{240} and Pu^{237}. These limits are considerably larger than the values of E_c calculated from the above $a\theta_0^2$ proportionality. Values of 11 and 15.2 MeV are calculated with values for Δ_k taken from Eq. (8) and from the paper of Nemirovsky and Adamchuk,[45] respectively. As pointed out by Griffin,[37] this indicates that the energy gap parameter for nuclei stretched to the saddle point is considerably greater than for the same nuclei in their equilibrium shape. Therefore, the 16-MeV value of E_c used for the thorium nuclides in the present anisotropy calculations, although chosen somewhat arbitrarily, is probably correct to within ± 5 MeV.

[44] H. K. Vonach, R. Vandenbosch, and J. R. Huizenga (to be published).

[45] P. E. Nemirovsky and Yu. V. Adamchuk, Nucl. Phys. 39, 551 (1962).

The present experimental data and anisotropy calculations do not obviate some other dependence of K_0 upon E at low excitation energies; for example, $K_0^2 \propto E^2$. It is clear that a more refined program is needed to ascertain a more quantitative description of the K_0^2 versus E distribution, a program in which the initial simplifying assumptions are replaced by more realistic ones and in which a best fit to the experimental data can be sought.

Fission fragment anisotropies induced in radium by deuterons do not exhibit large fluctuations as a function of bombardment energy (Fig. 1). This may result from a number of reasons. (1) The incoming deuterons provide less angular momentum to compound nuclei of the same excitation energy than do helium ions. (2) The angular momentum of the compound nucleus is not sharply aligned with deuterons because of the contribution of the intrinsic spin of the deuteron to the total angular momentum. This effect is relatively small. (3) Deuteron-induced fission at the energies investigated is primarily first- or second-chance fission. This is illustrated with the aid of Fig. 8. A captured 21-MeV deuteron excites a Ra^{226} target nucleus to approximately 29 MeV. As the excited Ac^{228} nucleus de-excites by neutron evaporation to an energy where third-chance fission becomes possible (an excitation energy of <11 MeV), fission becomes a very improbable process compared to the total reaction cross section because the Γ_n/Γ_f energy dependence is very steep for actinium nuclei. Consequently, the fission that does occur, does so at high excitation energies where the fission fragment anisotropy is expected to be low.

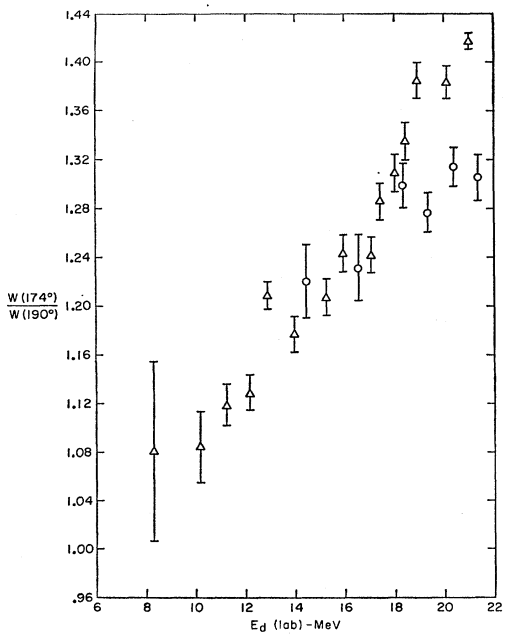

FIG. 12. Deuteron-induced fission fragment anisotropy from radium (circles) and thorium (triangles) as a function of projectile energy. The thorium data are from Ref. 3.

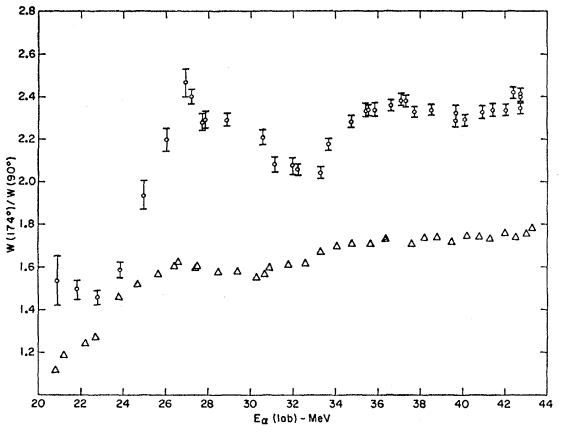

FIG. 13. Helium-ion-induced fission fragment anisotropy from radium (circles) and thorium (triangles) as a function of projectile energy. The thorium data are from Ref. 5.

This last reason then helps to explain the so-called "radium anomaly" in fission fragment anisotropy[1–4] mentioned in the Introduction. In deuteron-induced fission a thorium target nucleus has a much better chance of undergoing second- and third-chance fission than does a radium target nucleus. Since later-chance fission events are associated with large anisotropies (because of lower excitation energy) thorium might be expected to have a larger anisotropy with 21-MeV deuterons than radium.

In helium-ion-induced fission, however, radium has a large probability for third-, fourth-, and even fifth-chance fission occurring with 43-MeV helium ions. Since the U^{236} compound nucleus ($Th^{232}+He^4$) has a smaller Γ_n/Γ_f ratio than does the Th^{230} compound nucleus ($Ra^{226}+He^4$), the probability of first-chance fission is greater for thorium excited with 43-MeV helium ions than for radium. As a result, more fission occurs at higher excitation energies in thorium target nuclei than in radium target nuclei. Consequently, less anisotropy is expected with thorium than with radium.

The above interpretation of the observed radium fission fragment anisotropies assumes that the effective moments of inertia of the various nuclides involved vary in a regular manner according to the predictions of Cohen and Swiatecki[42] and Strutinskii *et al.*[43]

The magnitude of the "radium anomaly," according to the above interpretation, should depend upon the bombarding energies of the deuterons and helium ions at which the anisotropy is measured. This statement is realized and is illustrated with the aid of Figs. 12 and 13. In these two figures the anisotropies of both radium and thorium target nuclei are plotted as a function of deuteron and helium ion energy, respectively.

ACKNOWLEDGMENTS

The authors wish to acknowledge the members of the Argonne 60-in. cyclotron group who assisted in the arrangement of equipment and who operated the cyclotron during the many experimental runs involved. We wish also to thank Carl Ahlberg who assisted in many phases of this investigation, Dale Henderson who analyzed the alpha activities of the radium target, and members of the Radiation Safety Group for their constant vigilance. Editorial comments by Dr. James J. Griffin and Dr. Robert Vandenbosch have been greatly appreciated.